IEEE Access
Multidisciplinary | Rapid Review | Open Access Journal

Received September 24, 2019, accepted October 15, 2019, date of publication October 17, 2019, date of current version October 30, 2019.

Digital Object Identifier 10.1109/ACCESS.2019.2948196

An Optimization Strategy Based on Dimension Reduction Method in Wireless Charging System Design

LINLIN TAN[1,2], ZONGYAO TANG[1], RUYING ZHONG[1], XUELIANG HUANG[1,2], HAN LIU[1], AND CHEN CHEN[3]

[1]School of Electrical Engineering, Southeast University, Nanjing 210096, China
[2]Key Laboratory of Smart Grid Technology and Equipment in Jiangsu Province, Zhenjiang 212000, China
[3]Economic Research Institute, State Grid Jiangsu Electric Power Company Ltd., Nanjing 210000, China

Corresponding author: Linlin Tan (tanlinlin@seu.edu.cn)

This work was supported by the Science and Technology Project of State Grid Corporation of China through Wireless Charging Frequency Selection of Electric Vehicles and Its Impact on the Environment under Grant SGHB0000KXJS1800405.

ABSTRACT This study proposes an optimization strategy, which is based on a dimension reduction method with sensitivity analysis, for fast multi-objective optimization of coil design in the wireless power transmission (WPT) system. The multi-objective optimization process of coil in WPT usually involves general genetic algorithm (GA) and derivatives that suffer from common problems of slow search speed and heavy calculation burden, especially in the presence of multiple optimization variables. Moreover, in a complicated WPT system with ferrite, the optimization objective, such as the coupling factor k, is difficult to calculate analytically; in practice, it is acquired numerically using the finite element method (FEM), which also adds to the optimization complexity and time consumption. As a remedy, we propose the new strategy by simplifying the original complex optimization problem firstly with sensitivity assessment, and then applying NSGA-II convergence algorithm for optimization. Firstly, the optimization strategy is introduced, including the evaluation method, dimension reduction method and entire multi-objective optimization process. Then the optimization strategy is implemented to optimize the design parameters of a coil system. The sensitivity of design parameters is assessed with FEM analysis to realize the dimension reduction, and the optimization framework is established. Afterwards, the high sensitivity parameters will be optimized utilizing the multi-objective algorithm to obtain the optimal parameters. The simulation results demonstrate that, compared to the traditional NSGA-II algorithm, the proposed strategy yields a 44% reduction in the iteration time required for system convergence. Furthermore, the good agreement between the simulation and the measured sensitivity data and optimal parameters presents additional validation for the optimization strategy. The experiment further shows that implementation of the proposed strategy could lead to an increase in the maximum efficiency of the WPT system from 79.85% to 93.2%.

INDEX TERMS Wireless power transfer, coil design and optimization, sensitivity analysis, dimension reduction, time consumption reduction.

I. INTRODUCTION

In recent years, wireless power transmission (WPT) technology has developed rapidly and is being applied to numerous industries. The magnetically coupled resonant WPT technology proposed by the MIT research group provides advanced research frameworks for the energy transmission of medium-range. Compared with the traditional WPT system, the resonant WPT system has the advantages of high coupling coefficient and small electromagnetic field leakage value, etc. The critical factor to the feasibility of medium-range energy is a pair of coils with the same resonant frequency [1]–[3]. Efficient resonance coil design and optimization work therefore become the indispensable trend of WPT research [4]–[6]. Therefore, high efficiency in coil design must be one of the design goals. Since the coil system utilize electromagnetic field to transmit energy, the exposure value of electromagnetic field to the human body will also increase with the

The associate editor coordinating the review of this manuscript and approving it for publication was Mehmet Alper Uslu.

improvement of WPT power level. However, WPT system may pose a potential biological threat to adults, children and pregnant women, which is reflected in the electromagnetic field (EMF) induced by the human body and the electromagnetic wave specific absorption rate (SAR) of the organism. High EMF and SAR values will lead to severe local fever in human tissues and even injury to human tissue structure [7]–[10], hence it is necessary to append human electromagnetic safety into the optimization objective of coil design.

Considering the complexity in coil design, it is a multi-objective and multi-parameter problem which is usually solved by using intelligence algorithm such as genetic algorithm (GA) or particle swarm optimization (PSO). In the past researches, there are some studies adopting the GA or PSO method to solve the related problems in WPT systems. In the field of algorithms, the evaluation of different algorithms was mainly based on two factors: 1. Its optimization performance. 2. Its complexity or time spent [11], [12]. Reference [12] systematically introduced a fast and elitist multi-objective genetic algorithm (NSGA-II). The algorithm had better convergence performance at the optimal solution, and is faster compared with NSGA-I in [11], which has been widely recognized and applied. Reference [13] used the GA method to optimize five circuit parameters based on improving the coupling coefficient of the coil. Nevertheless, it did not discuss about the time consumption and its optimization performance. Reference [14] adopted the GA method to modify sixteen parameters of the receiving resonator array to ameliorate the power transmission efficiency and misalignment of coil. It only paid attention to the optimization performance but neglect the time comparison. In [15], the particle swarm optimization (PSO) method was adopted to optimize five design parameters in the magnetic links of WPT system and yielded good performance. Moreover, the time-consuming design parameters combinations were simplified, but it still needed 1000 iteration computations. Reference [16] improved the PSO method to reduce the optimization parameters in circular WPT couplers. The eleven parameters were reduced to six parameters, and the time cost was reduced under the same optimization performance. Therefore, regardless of the intelligent optimization method, the number of optimization parameters is one of the important factors in determining the complexity and time consumption of the optimization process. Reducing the number of optimization parameters using the sensitivity analysis can reduce optimization time consumption exponentially. Moreover, reference [17] indicated that when a low sensitivity parameter fluctuates towards the optimal parameters, the convergence speed of the optimization target may be slower, and even divergence may occur. If sensitivity analysis is implemented before optimization design, it can not only distinctly reduce the computational workload and improve work efficiency, but also further enhance the engineering guiding significance of optimization design [18]–[20]. In addition, good optimizing performance can not be ignored either.

In these past researches, up to dozens of optimization parameters were substituted into the optimization algorithms, while the problem of time consumption have been ignored. This might be owing to the availability of clear analytical formula for the optimization objective as well as the help of powerful computing tools such as MATLAB. In a practical WPT system, the coils are usually fitted with ferrite and aluminum plates, and it is difficult to calculate system related indicators such as the human induced electromagnetic field to be optimized in this paper, which will undoubtedly increase the time required for iteration. Therefore, it would be cumbersome and time-consuming to employ those previous methods which depend on many iterations to converge. This paper proposes an optimization strategy based on dimension reduction method. The strategy first simplifies the complex optimization problem by utilizing the sensitivity analysis, and then performs optimization with mature algorithm, i.e. the fast and elitist multi-objective genetic algorithm (NSGA-II), for coil design. Compared to previous researches, the contribution of this paper is two folds. Firstly, the optimization strategy is capable of reducing the iterations and time consumption required for WPT system optimization. Secondly, the optimization strategy a good improvement effect on the system performance(system objectives), and the performance loss is within acceptable limits. Moreover, the strategy of this paper has guiding significance for faster and good WPT engineering design.

The rest of the paper is arranged as follows. In section II, the optimization strategy models including the evaluation model, dimension reduction model and multi-objective optimization model are introduced. In Section III, the optimization strategy is implemented to optimize design parameters of a coil system in the simulation, including the optimization process in detail. The optimization results are obtained and discussed. Section IV is the physical system and experimental verification. The correctness of the sensitivity analysis result and the optimal parameters of the optimization strategy are verified by experiments. Section V is the conclusion.

II. OPTIMIZATION STRATEGY MODEL

This section mainly introduces the entire optimization strategy, including the evaluation model, dimension reduction model and multi-objective optimization model. The evaluation model mainly introduces the source of the two optimization objectives to be optimized in WPT system. The dimension reduction model mainly introduces the sensitivity analysis method. Multi-objective optimization model mainly introduce the detailed process of the optimization strategy in this paper, including fitness function, penalty function and complete iterative process.

A. EVALUATION MODEL

According to the descriptions in introduction, the high efficiency of WPT system and high human electromagnetic safety are two optimization objectives. The objectives need to be evaluated by corresponding parameters.

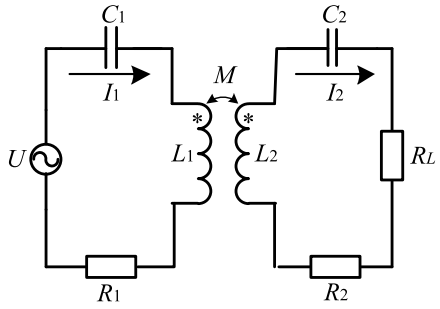

FIGURE 1. WPT system circuit using a lumped parameter model.

Typical energy transmission process of a WPT system is as follows: The high-frequency electric energy is applied to transmitter coil from the AC power source. Subsequently, the energy is transmitted to the load side (secondary side) through LC compensation topology and transmitter and receiver coils. The energy transmitted from the primary side is employed to charge the load through LC compensation topology [21], [22]. In the practical application on vehicle of WPT system, the receiver coil is mostly loaded on the vehicle, and the transmitter coil is mostly installed under the ground with a certain energy transmission distance between them.

Figure 1 shows the equivalent circuit model of WPT system using lumped parameter model when using a series–series (SS) compensation topology.

In Figure 1, U represents the high frequency AC voltage source. C_1, L_1, R_1 represent primary capacitance, inductance, resistance and C_2, L_2, R_2 represent secondary capacitance, inductance, resistance respectively. I_1 and I_2 denote the primary and secondary current. M denote the mutual inductance of the transmitter and receiver coils. R_L denotes the equivalent resistance load. In an ideal analysis process, system is predetermined to operate at a resonance status. The equivalent KVL equations of the circuit can be written by using Kirchhoff's Law as follows:

$$\begin{cases} \dot{U} = R_1 I_1 - j\omega M \dot{I}_2 \\ j\omega M \dot{I}_1 = (R_2 + R_L)\dot{I}_2 \end{cases} \tag{1}$$

When the system coil resonates, the efficiency of the system η can be derived as follows:

$$\eta = \frac{R_L \times (\omega M)^2}{(R_2 + R_L)((\omega M)^2 + R_1(R_2 + R_L))} \tag{2}$$

We take the derivative of η with respect to R_L as follows:

$$\frac{\partial \eta}{\partial R_L} = (\omega M)^2 R_1 R_2^2 + (\omega M)^4 R_2 - (\omega M)^2 R_1 R_L^2 \tag{3}$$

The system efficiency is maximized when equation (3) equals to zero, so it can be derived that the optimal load $R_{L(\text{opt})}$ corresponding to the maximum efficiency can be obtained as follows:

$$R_{L(\text{opt})} = \sqrt{R_2^2 + (\omega M)^2 \frac{R_2}{R_1}} \tag{4}$$

The mutual inductance calculation equation is $M = k \times \sqrt{L_1 \times L_2}$, and the L_1 and L_2 are converted by the quality factor equation of the transmitter coil $Q_1 = \omega L_1/R_1$ and the quality factor equation of the receiver coil $Q_2 = \omega L_2/R_2$. Afterwards, the mutual inductance M in (4) is converted to $M = k^2 R_1 R_2 Q_1 Q_2$ and the optimal load $R_{L(\text{opt})}$ is changed as follows:

$$R_{L(\text{opt})} = \sqrt{1 + k^2 Q_1 Q_2} R_2 \tag{5}$$

The maximum efficiency $\eta_{\max}$ corresponding to the $R_{L(\text{opt})}$ is

$$\eta_{\max} = \frac{(\sqrt{1 + k^2 Q_1 Q_2} - 1)^2}{k^2 Q_1 Q_2} \tag{6}$$

When the transmitter and receiver coil are identical ($Q = Q_1 = Q_2$), the $k^2 Q_1 Q_2$ can be written as $(kQ)^2$. The equation (6) is simplified by regulating A equal the reciprocal of kQ, and we take the derivative of η_{max} with respect to A as follows:

$$\frac{\partial \eta_{\max}}{\partial A} = \frac{1}{\sqrt{1 + (\frac{1}{A})^2}} - 1 \tag{7}$$

According to equation (7), $\frac{\partial \eta_{\max}}{\partial A}$ is always less than zero, and $\eta_{\max}$ will increase with the decline of A parameter, that is, $\eta_{\max}$ increases with the increase of kQ_1Q_2, so it essentially demonstrates that the efficiency is not determined by k or Q alone but by their product. Therefore, if the kQ_1Q_2 parameter can be augmented by means of optimization, the maximum efficiency of the entire WPT system will ascend with reasonable load matching, so this paper assigns kQ_1Q_2 as the evaluation parameter of efficiency optimization.

For another optimization objective (high human electromagnetic safety), the internationally authoritative standards for human exposure to electromagnetic fields are ICNIRP 1998 [23] and ICNITP 2010 [24]. In ICNIRP 1998, the inductive electric field specific absorption rate (SAR) is mainly adopted for human body safety assessment while the human body induced electric field value is evaluated in ICNIRP 2010, so this paper takes the induced electric field value E in human tissue as another evaluation parameter.

Therefore, we can evaluate the coil design by calculating these two evaluation parameters. The specific evaluation equation which is called the fitness function will be shown in Section II C.

B. DIMENSION REDUCTION MODEL

During the iteration process of the population in genetic algorithm, the optimization parameters of each individual in the population will mutate just as humans produce genetic mutation in the next generation. At this point, if the parameters with low sensitivity mutated, the new individual will not have a good improvement performance on the optimization objectives, and mutation is meaningless. If multiple optimization parameters mutated in a meaningless way, the number of iterations and time consumption required for system convergence will eventually increase. On the contrary, if the high

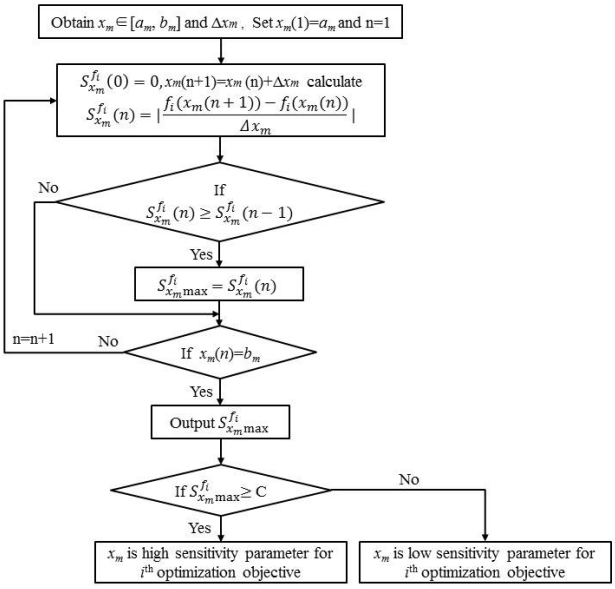

FIGURE 2. The flowchart of the sensitivity analysis.

sensitivity parameters in design parameters of WPT system are pick out to become the optimization parameters, and the low-sensitivity parameters are eliminated, every mutation of optimization parameters will be effective, which will accelerate the iteration to the optimal parameters and obviously reduce the time consumption.

Sensitivity analysis is generally divided into global sensitivity analysis and local sensitivity analysis. Global sensitivity indices should be regarded as a tool for studying the mathematical model rather than its specified solution [25] while local sensitivity is mainly adopted to evaluate the influence of change of a single parameter exerting on optimization objective, and local sensitivity is principally used to settle engineering problems. Assuming that there are initially m design parameters to be optimized, measurement method of local sensitivity is

$$S_{x_m}^{f_i} = \left| \frac{\partial f_i(x_m)}{\partial x_m} \right| \tag{8}$$

where $f_i(x_m)$ represents the value of i^{th} optimization objective and x_m represents the m^{th} design parameter in an individual of a population. Every design parameter x_m has a variation range $[a_m, b_m]$ and the reasonable step size is set as Δx_m. The maximum sensitivity value $S_{x_m \max}^{f_i}$ which is obtained by Figure 2 will be taken as the sensitivity measurement index.

The high sensitivity design parameters will be determined to be the optimization parameters according to the criterion as follows:

$$S_{x_m \max}^{f_i} \geq \mathrm{C} \tag{9}$$

The C is a constant value and its specific value is depended on the situation. The detailed sensitivity analysis process of design parameters is as follows:

Step I: Obtain the variation range $[a_m, b_m]$ of design parameter x_m and set $x_m(1) = a_m$, n = 1.

Step II: $x_m(n+1) = x_m(n) + \Delta x_m$ and calculate $S_{x_m}^{f_i}(n) = \left|\frac{f_i(x_m(n+1))-f_i(x_m(n))}{\Delta x_m}\right|$ utilizing equation (8).

Step III: Set $S_{x_m}^{f_i}(0) = 0$. If $S_{x_m}^{f_i}(n) \geq S_{x_m}^{f_i}(n-1)$, the maximum sensitivity value $S_{x_m \max}^{f_i} = S_{x_m}^{f_i}(n)$ else it goes to the step IV.

Step IV: If $x_m(n) = b_m$, output $S_{x_m \max}^{f_i}$, else set n = n + 1 and return to step II.

Step V: Determine whether the design parameter x_{m} is high sensitivity design parameter by equation (9).

Figure 2 shows the flowchart of the sensitivity analysis employed in this paper. Every optimization objective will generate several high sensitivity optimization parameters with the corresponding restriction C. The ultimate optimization parameters are their intersection. Therefore, the high sensitivity design parameters become optimization parameters and the low sensitivity design parameters will be fixed to a constant parameter and eliminated from the iteration process.

C. MULTI-OBJECTIVE OPTIMIZATION MODEL

For two optimization objectives in this article, classical optimization methods convert the multi-objective optimization problem to a single-objective optimization problem by setting one particular Pareto-optimal solution [26]. NSGA-II similarly uses the Pareto-optimal solution. The Pareto-optimal solution mainly use the fitness function(also called the Pareto non-dominated front) to judge the optimization results. The differences between NSGA-II and other algorithms are the fast non-dominated sorting approach and the import of crowded-comparison approach. NSGA-II has faster optimization speed and preserves the diversity among population members with a better computational complexity [27]. Therefore, this paper adopts NSGA-II algorithm as an example to verify the optimization strategy for the coil design system.

The main fitness function and punish function are introduced in the following and the identical procedures in NSGA-II such as the procedure of fast non-dominated sort and crowding distance calculation are omitted.

It is assumed that there are N individuals in the initial population. $\boldsymbol{x_{j(ori)}}$ (vector) represents the j^{th} original individual composed of m design parameters $x_{m(\text{ori})}$ before dimension reduction and can be expressed by

$$\overrightarrow{x_{j(\text{ori})}} = (x_{1(\text{ori})}, x_{2(\text{ori})}, \ldots, x_{m(\text{ori})})_j, \quad j = 1, \ldots, N \tag{10}$$

where m denotes the dimension of $\boldsymbol{x_{j(ori)}}$. The optimization parameters' dimension of $\boldsymbol{x_{j(ori)}}$ can be reduced by using the sensitivity analysis of dimension reduction model. High sensitivity parameters are selected and extracted for subsequent optimization. Then the new individual $\boldsymbol{x_j}$ is obtained and expressed by

$$\overrightarrow{x_j} = (x_1, x_2, \ldots, x_{m'})_j, \quad j = 1, \ldots, N \tag{11}$$

where m' denotes the dimension of $\boldsymbol{x_j}$. In this paper, high efficiency of the WPT system and high human electromagnetic safety are the optimization objectives which are evaluated by calculating parameters kQ_1Q_2 and E. Due to the

unavailability of clear analytical formula for kQ_1Q_2 and E, the calculation function $f_{1j}(\boldsymbol{x_j})(j = 1 \text{ to } N)$ are defined to represent the result of kQ_1Q_2 when substituting the j^{th} individual $\boldsymbol{x_j}$ into calculation. The calculation function $f_{2j}(\boldsymbol{x_j})$ is also defined to represent the result of E. The larger value of $f_{1j}(\boldsymbol{x_j})$ signifies the higher transmission efficiency of the system while the smaller value of $f_{2j}(\boldsymbol{x_j})$ brings the higher safety of human EMF, which means the two objectives have incompatibility features. Therefore, the $f_{2j}(\boldsymbol{x_j})$ is replaced by $f'_{2j}(\boldsymbol{x_j})$ as(12), and the $f'_{2j}(\boldsymbol{x_j})$ and $f_{1j}(\boldsymbol{x_j})$ have the consistent optimization direction.

$$f'_{2j(\overrightarrow{x_j})} = \frac{1}{f_{2j(\overrightarrow{x_j})}}, \quad j = 1, \ldots, N \tag{12}$$

$f_1^{\max}$ and $f_2^{\max'}$ are the max value of $f_{1j}(\boldsymbol{x_j})$ and $f'_{2j}(\boldsymbol{x_j})$ written as follows:

$$\begin{aligned} f_1^{\max} &= \max(f_{11(\overrightarrow{x_1})}, f_{12(\overrightarrow{x_2})}, \ldots, f_{1N(\overrightarrow{x_N})}) \\ f_2^{\max'} &= \max(f_{21(\overrightarrow{x_1})}, f_{22(\overrightarrow{x_2})}, \ldots, f_{2N(\overrightarrow{x_N})}) \end{aligned} \tag{13}$$

The fitness function F_j of j^{th} new individual is established to judge the optimization results as follows:

$$F_j = w_1 \times \frac{f_{1j(\overrightarrow{x_j})}}{f_1^{\max}} + w_2 \times \frac{f'_{2j(\overrightarrow{x_j})}}{f_2^{\max'}}, \quad j = 1, \ldots, N \tag{14}$$

where the ω_1 and $\omega_2(\omega_1 + \omega_2 = 1)$ are measure factors determined by the degree of emphasis on kQ_1Q_2 and E.

According to ICNITP 2010 [24], the human body induced electric field value E is required to be lower than 135V/m, which means the value of $f_{2j}(\boldsymbol{x_j})$ should be lower than 135V/m. The D is use to represent this constant value. The optimization model of the system is built as follows:

$$\begin{cases} \max\ F_j = w_1 \times \dfrac{f_{1j(\overrightarrow{x_j})}}{f_1^{\max}} + w_2 \times \dfrac{f'_{2j(\overrightarrow{x_j})}}{f_2^{\max'}}, & j = 1, \ldots, N \\ \text{s.t.}\ f_{2j(\overrightarrow{x_j})} \le \text{D}, & j = 1, \ldots, N \\ a_n \le x_n \le b_n, & n = 1, \ldots, k' \end{cases} \tag{15}$$

where the a_{n} and b_{n} are the constant limiting values for optimization parameter x_{n} determined by engineering experience or circumstance.

Due to the restriction of $f_{2j}(\boldsymbol{x_j})$, the penalty function pf_j is built as (16) to convert constrained optimization to unconstrained optimization.

$$\Delta f_{2j(\overrightarrow{x_j})} = \begin{cases} \left| f_{2j(\overrightarrow{x_j})} - \text{D} \right|, & f_{2j(\overrightarrow{x_j})} > D \\ 0, & f_{2j(\overrightarrow{x_j})} \le D \end{cases} j = 1, \ldots, N \tag{16}$$

$$\max \Delta f_2 = \max(\Delta f_{21(\overrightarrow{x_1})}, \Delta f_{22(\overrightarrow{x_2})}, \ldots, \Delta f_{2N(\overrightarrow{x_N})}) \tag{17}$$

$$pf_j = \begin{cases} 1 - \dfrac{\Delta f_{2j(\overrightarrow{x_j})}}{\max \Delta f_2}, & \max \Delta f_2 > 0 \\ 1, & \max \Delta f_2 = 0 \end{cases} j = 1, \ldots, N \tag{18}$$

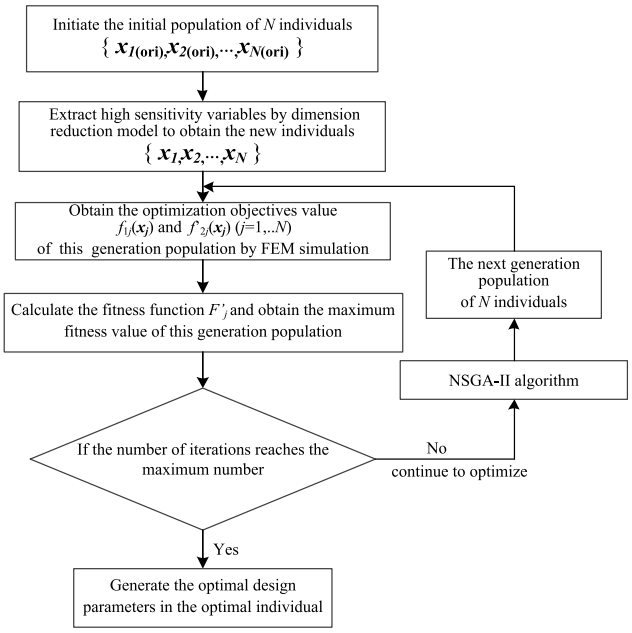

FIGURE 3. The optimization strategy for multi-objective optimization.

The new fitness function F'_j is

$$F'_j = F_j \times pf_j, \quad j = 1, \ldots, N \tag{19}$$

The equations (16)-(18) demonstrate that if the value of $f_{2j}(\boldsymbol{x_j})$ exceeds the restriction D, the value of fitness function will be multiplied by a factor pf_{j} less than 1 as a penalty. Otherwise, the value of pf_{j} is 1, which means the fitness will not change.

The final optimization model of the system is built as follows:

$$\begin{cases} \max\ F'_j = pf_j \\ \times (w_1 \times \dfrac{f_{1j(\overrightarrow{x_j})}}{f_1^{\max}} + w_2 \times \dfrac{f'_{2j(\overrightarrow{x_j})}}{f_2^{\max'}}), & j = 1, \ldots, N \\ \text{s.t.}\ a_n \le x_n \le b_n, & n = 1, \ldots, k' \end{cases} \tag{20}$$

After building the optimization model, the optimization performance will be evaluated by the maximum F'_j. The larger the maximum fitness value is, the better the optimization performance of this population generation is. Until the number of iterations reaches the maximum number, the current generation population will generate the next generation population of the same number individuals through the NSGA-II algorithm including fast non-dominated front sorting, crowding distance sorting, selection, crossover and mutation. Due to the same procedures, it is not described in detail in this paper. The integrated optimization procedure used in this paper is shown in Figure 3.

The two objectives without an explicit formula can be optimized through the above strategy, and the dimension reduction can accelerate the iterative procedure, which will be verified by the following implementation of the optimization strategy and experiments.

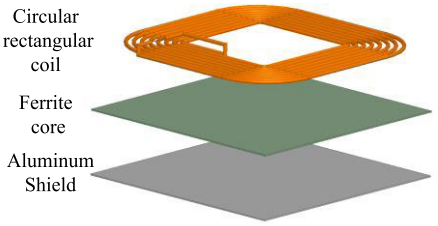

FIGURE 4. Transmitter circular coil system to be optimized (receiver coil is the same).

TABLE 1. Basic parameters of the coil model to be optimized.

Object	Parameters	Value
Coil	external diameters length (a_1)	360 mm
	external diameters width (a_2)	360 mm
	turn spacing (d)	12 mm
	coil turns (n)	8
	radius of wire (a)	2.5mm
	coil spacing (Z_1)	190mm
Ferrite	length (b_1)	360 mm
	width (b_2)	360 mm
	thickness (b_3)	2 mm
	distance from coil (Z_2)	0.1 mm
Aluminum shield	length (b_1)	360mm
	width (b_2)	360mm
	thickness (b_3)	2mm

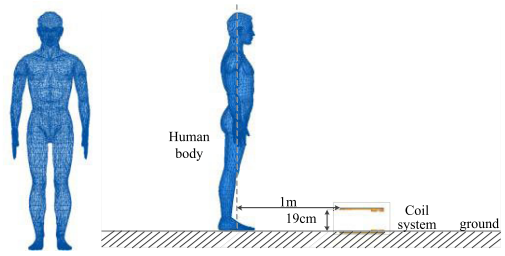

(a) Human body system (b) Relative positional relationship

FIGURE 5. The simulation test setup of coil and human body system.

III. IMPLEMENTATION OF OPTIMIZATION STRATEGY

A. BACKGROUND OF OPTIMIZATION

Figure 4 shows the magnetically coupled coil model to be optimized in this paper. It is established by referring to the SAE J2954 rounded rectangular coil system [28]. The four corners of the rounded rectangular coil are circular arc which possessed better characteristics under the offset condition than the circular coil and the leakage flux in edge is modified compared to the corner of the rectangular coil [29]. In addition to the coil itself, the model is fabricated with a ferrite core and an aluminum plate around the coil according to [28]. The aluminum shield plate is the same size as the ferrite core and fit the ferrite distribution. The basic values of parameters in coil model, ferrite and aluminum plate nearly imitate the WPT2/Z2 circular rectangular coil's dimensions in SAE J2954 including the length, width, coil turns, radius of wire and so on. Specific dimensions are shown in Table 1.

Figure 5 shows the human body model structured in the simulation and the relative position of the human body to the coil. The simulation adopts a 30-year-old middle-aged male human body model with a height of 175cm and a weight of 70kg. Assuming that the coil is applied to an electric vehicle and the transmitter coil is buried in the ground, normally speaking, the person should be placed in the vehicle and the coil is placed at the bottom of the car. However, according to our laboratory test, when the human body is placed in the car, the human body induced electric field is far less than the limit due to the shielding performance of the metal material in the car body. In addition, this paper mainly focuses on static wireless charging. In the process of static wireless charging, the human body is mostly distributed outside the vehicle. Therefore, this article considers the condition of more serious electromagnetic radiation, that is, the human body is placed at a position 1m away from the coil to make the optimization results can guarantee the safety of the human body furthest. The human foot surface can be set flush with the transmitter coil as Figure 5(b).

TABLE 2. Electromagnetic parameters of the system materials.

Object	Relative permittivity	Relative Permeability	Bulk Conductivity
Copper	1	0.99991	58000000 s/m
Ferrite	12	3300	0.01 s/m
Aluminum	1	1.000021	38000000 s/m
Human	1120	1	0.00388 s/m

Two optimization objectives need to be observed simultaneously. In simulation part, the input voltage of the primary side is constant. The working frequency is set to 85 kHz, and 85 kHz is a generally resonant frequency accepted by the SAE [28], IEC [30] and ISO [31] standards. The choice of the frequency does not affect our optimization and results. Electromagnetic parameters of each material are tabulated in Table 2.

B. THE DETAILED OPTIMIZATION PROCESS USING OPTIMIZATION STRATEGY

The optimization process is performed in strict accordance with the procedures in Figure 3.

1) THE INITIAL POPULATION

Assuming that the initial population is composed of 60 individuals, every individual is composed of several design parameters to be optimized in WPT coil design. The design parameters and their variation range are required to determine firstly.

According to the electromagnetic field theory, the magnitude of the electromagnetic field around the coil system is directly related to the coil current value, and is greatly affected by the current. In the case of external circuit confirmation, modulating the coil parameters should not affect its conduction current which indicates the coil resistance should not be altered. Therefore, the length of the coil should not be altered, which means that the length and width of the coil

TABLE 3. The design parameters of the coils to be optimized and their restrictions.

Design parameters	Restrictions
turn spacing : d	[10mm,12mm]
coil spacing: Z_1	[170mm,210mm]
length of ferrite(aluminum shield): b_1	[340mm,380mm]
width of ferrite(aluminum shield): b_2	[340mm,380mm]
thickness of ferrite(aluminum shield): b_3	[1mm,5mm]
distance of ferrite from coil (Z_2)	[0.1mm,5mm]

model a_1, a_2 and the number of turns n can not become design parameters. The coil turns spacing d, the distance between transmitter and receiver coils Z_1, the length, width and height of the ferrite and aluminum shield $b_1 \sim b_3$, and the distance between coil and ferrite Z_2 are design parameters to be optimized. Based on the reference [28]–[31] and practical experience, the optimization parameters have their own limitations. The spacing of the coil turns can be determined according to the length and width of the wire, the number of turns, the radius and the edge of the arc combined with the actual winding frame. The $b_1 \sim b_3$ and Z_2 should be allocated to a reasonable range based on the engineering foundation. All the design parameters of the coils and their restrictions are shown in Table 3.

The initial population is composed of the 60 individuals $\boldsymbol{x_{j(ori)}}$ as follows:

$$\overrightarrow{x_{j(\mathrm{ori})}} = (d, Z_1, b_1, b_2, b_3, Z_2)_j, \quad j = 1, \ldots, 60 \qquad (21)$$

2) THE NEW INDIVIDUALS AFTER DIMENSION REDUCTION

Before implementing the sensitivity analysis to realize dimension reduction, in order to make the simulation and experiment comparable, this paper decides to designate a base value Q_{N} to replace the value of optimization objective kQ_1Q_2 corresponding to the base size of coil system in Table 1. All subsequent sensitivity analysis results of kQ_1Q_2 will be compared with the Q_{N}. For another optimization objective (human electromagnetic safety), the value measured at base size is also designated as the base value E_{N}, and all subsequent sensitivity analysis results of E will be compared with E_{N}. The later experimental verification section adopts define the same Q_{N} and E_{N}. In this way, the simulation results can be compared with the experimental results in the same range to verify the consistency of relevant results.

Sensitivity analysis is performed utilizing ANSYS finite element (FEM) electromagnetic analysis software. The analysis tests are carried out under the experimental conditions of Figure 4-5 and Table 1. The value of kQ_1Q_2 under each design parameter is calculated for sensitivity analysis.

Figure 6 is human induced electric field diagram of the human body surface under the basic parameters in Table 1, and other similar diagrams are not displayed. It can be visually interpreted from the image color distribution that the electric field of the human body presents high induced values on both sides of the waist, on both sides of the shoulder and

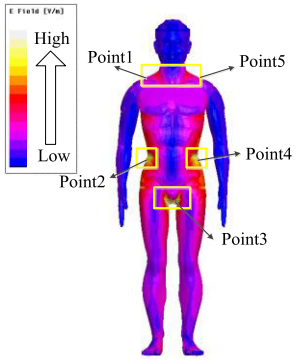

FIGURE 6. The simulation test setup of coil and human body system.

in the genital area, and the waist and genital area present the highest induced value while the shoulder is slightly low. Due to the demand to observe whether the electric field intensity satisfies restrictions, the test points are set in these areas presenting higher induced values, which are marked point 1-5 in Figure 6. The induced electric field value corresponding to the point under the basic experimental conditions is taken as the base value E_{N}, and the human induced electric field value E under each design parameter is tested and the sensitivity analysis is carried out.

The sensitivity analysis of kQ_1Q_2 corresponding to each design parameter is plotted separately as Figure 7(a)-(f) and E corresponding to each design parameter is shown in Figure 8(a)-(f).

The maximum sensitivity $S^{fi}_{x_k\,\max}$ is obtained by Figure 2, Figure 7(a)-(f) and Figure 8(a)-(f). According to Figure 7, the optimization objective kQ_1Q_2 is basically inversely proportional to the parameters d, Z_1 and Z_2, and the maximum sensitivity corresponds to $0.1225\ Q_{\mathrm{N}}$/mm, $0.0142Q_{\mathrm{N}}$/mm and $0.0399Q_{\mathrm{N}}$/mm respectively. Inversely, kQ_1Q_2 is basically proportional to the parameters b_1, b_2 and b_3, and the corresponding maximum sensitivities are $0.0449Q_{\mathrm{N}}$/mm, $0.0093Q_{\mathrm{N}}$/mm and $0.0083Q_{\mathrm{N}}$/mm respectively.

It can be demonstrated from Figure 8 that the human body induced electric field intensity E presents a large value at point 2 and point 4 and fluctuates significantly. At the optimization parameters d, Z_1, Z_2 and b_2, the maximum sensitivity $S^{fi}_{x_k\,\max}$ appears at point 2, which corresponds to $3.5928E_{\mathrm{N}}$/mm, $0.215E_{\mathrm{N}}$/mm, $1.748E_{\mathrm{N}}$/mm and $0.3829E_{\mathrm{N}}$/mm respectively. At the optimization parameters b_1 and b_3, the maximum sensitivity $S^{fi}_{x_k\,\max}$ appears at point 4, which corresponds to $0.248E_{\mathrm{N}}$/mm and $0.834E_{\mathrm{N}}$/mm respectively.

Based on equation (9), the value of C for optimization objective kQ_1Q_2 is defined as $0.03Q_{\mathrm{N}}$/mm, and the value of C for E is defined as $0.5E_{\mathrm{N}}$/mm. Therefore, comparing the value of maximum sensitivity with the corresponding restriction C, it can be obtained that the high sensitivity parameters for kQ_1Q_2 are d, Z_2 and b_1, and the high sensitivity parameters for E are d, b_3 and Z_2. Colligating the intersection of the sensitivity analysis results of kQ_1Q_2 and E, the pivotal optimization parameters are d and Z_2, and the values of

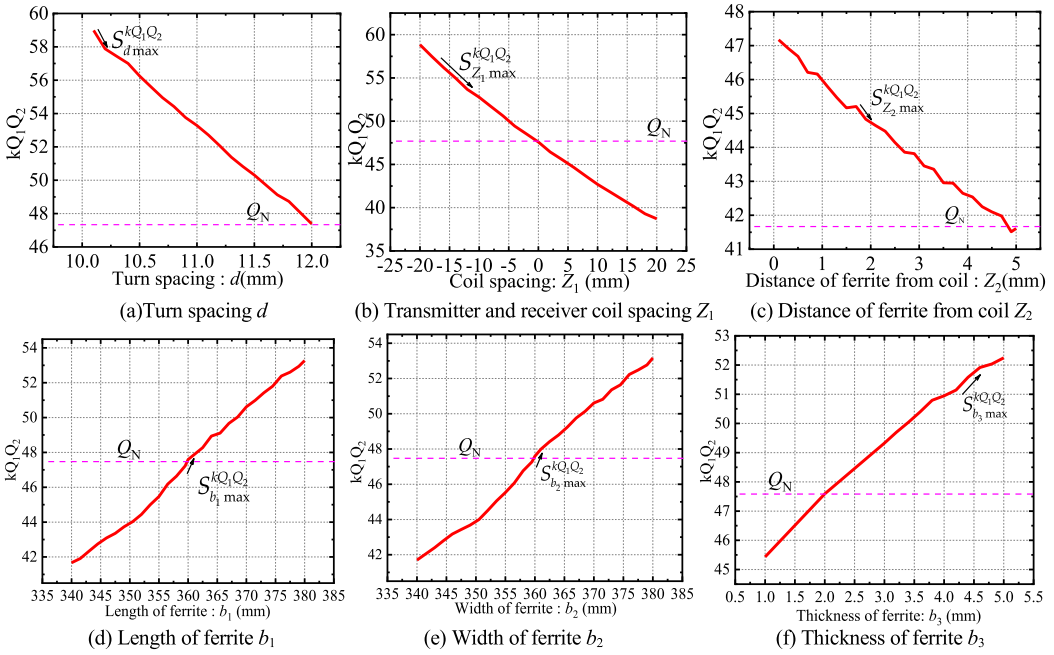

FIGURE 7. Optimization objective kQ_1Q_2 sensitivity analysis result corresponding to each design parameter.

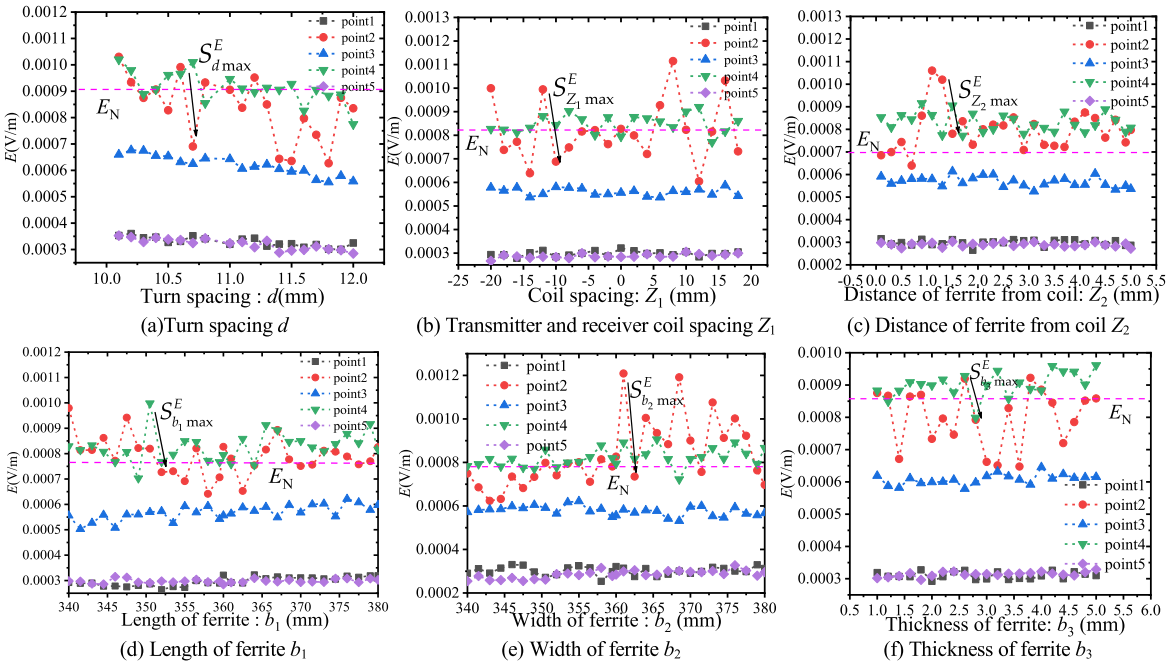

FIGURE 8. Optimization objective E sensitivity analysis result corresponding to each design parameter.

design parameters with low sensitivity are fixed as Table 1. So far, dimension reduction process has been accomplished. The new individual $\boldsymbol{x_j}$ composed of optimization parameters after dimension reduction is

$$\overrightarrow{x_j} = (d, Z_2)_j, \quad j = 1, \ldots, 60 \tag{22}$$

3) THE FITNESS FUNCTION CALCULATION

The new individuals $\overrightarrow{x_j} = (d, Z_2)_j$ in the current generation will be substituted into the ANSYS FEM simulation of coil system, and the values of kQ_1Q_2 will be obtained as $f_{1j}(\boldsymbol{x_j})(j = 1 \text{ to } N)$. According to the discussion of Figure 8, the maximum sensitivity appears more at point 2, hence the value of E in point 2 will be taken as objectives value $f_{2j}(\boldsymbol{x_j})$ of E.

In equation (14), the w_1 and w_2 are determined by the degree of emphasis on kQ_1Q_2 and E. It is observed that the objectives value E is much less than the limiting value D, so the kQ_1Q_2 is relatively more important than E. Based on the above analysis, the w_1 and w_2 are defined as 0.7 and

0.3. The fitness function F'_j of the j^{th} individual in current generation is

$$F'_j = pf_j \times (0.7 \times \frac{f_{1j((d,Z_2)_j)}}{f_1^{\max}} + 0.3 \times \frac{f'_{2j((d,Z_2)_j)}}{f_2^{\max'}}), \quad j = 1, \ldots, 60 \tag{23}$$

The calculation method of $f_1^{\max}$, $f_2^{\max'}$ and pf_j have been introduced in the equation (13)-(18).

The final multi-objective model of the simulation system is

$$\begin{cases} \max \ F'_j = pf_j \\ \times (\dfrac{0.7 f_{1j((d,Z_2)_j)}}{f_1^{\max}} + \dfrac{0.3 f'_{2j((d,Z_2)_j)}}{f_2^{\max'}}), \quad j = 1, \ldots, 60 \\ \text{s.t. } 10\text{mm} \le d \le 12\text{mm} \\ 0.1\text{mm} \le Z_2 \le 5\text{mm} \end{cases} \tag{24}$$

4) THE ITERATIVE PROCESSING OF OPTIMIZATION

After calculating the fitness value of all individuals in current generation, the maximum fitness value is obtained, and the current population generation will enter the NSGA-II iterative process to generate the next generation composed of 60 individuals until the number of iterative reaches the maximum value. In this paper, the maximum number of iterations is defined as 100. All iterative relevant algorithms are coded in MATLAB. When the iterations are complete, every maximum fitness value of every generation will be recorded to describe the process of system convergence. When the system converges, the optimal generation and optimal individual will be generated, and the parameters in the optimal individual will become the optimal optimization parameters. Combined with constant parameters, the optimal design parameters are obtained.

C. THE OPTIMIZATION RESULTS ANALYSIS

We perform 100 independent repeated experiments by using 100 random initial populations for our strategy test to realize relative good solution. The optimization results among these repeated experiments are all improved, but the improvement effect is slightly different. Therefore, we pick up the result with relative better improvement effect on the system performance and show it here.

Based on the implementation of the improvement strategy, the curve of convergence process is shown in Figure 9. The improvement effect on the system performance is evaluated by maximum fitness value. Afterwards, in order to highlight the rapidity and correctness of the improvement strategy in this paper, the improvement process is also executed by NSGA-II algorithm without the dimension reduction step. The initial population individuals with six improvement parameters as $\overrightarrow{x_{j(ori)}} = (d, Z_1, b_1, b_2, b_3, Z_2)_j$ are substituted in the improvement process. The convergence process of NSGA-II algorithm is also plotted in Figure 9. The convergence value of maximum fitness value and the corresponding ultimate design parameters are shown in Table 4.

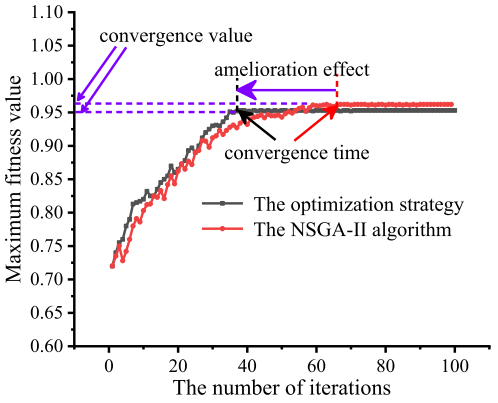

FIGURE 9. The curves of convergence process in the two conditions.

TABLE 4. The comparison of simulation results in the two conditions.

Condition	Convergence value of maximum fitness value	Convergence time	Optimal design parameters (d,Z1,b1,b2,b3,Z2) (unit: mm)
optimization strategy	0.953	at 38th iteration	(10.3,190,360, 360,5,0.4)
NSGA-II algorithm	0.962	at 68th iteration	(10.3,188.5,363.1, 362.8,5.3,0.4)

Comparing the two curves in Figure 8, the number of iterations required for system convergence increases several times without the dimension reduction step. Due to the limited number of individuals and the increase in the number of optimization parameters, the new individual after iteration may mutate in the low sensitivity parameters, which has slight performance on the fitness value evaluation. These similar mutation processes will slow down the convergence rate of the optimization parameters to the optimal value, which verifies the necessity of dimension reduction step. Considering the time requirements of the ANSYS FEM simulation, an iteration of an individual will consume plenty of time. Assuming that every iteration process consumes the same amount of time without taking the complexity of the extra parameters into consideration, the optimization strategy can reduce the number of iterations and iteration time required for system convergence by nearly 44%. The comparison of the convergence time in Table 4 verifies that the optimization strategy has successfully simplified the optimization problem by reducing the iterations and time consumption required for system convergence, which is one of the key contributions of this study.

On the other hand, the optimizing performance should be taken into consideration. Since the optimization problem has been simplified, the optimization performance would inevitably be affected. However, Table 4 shows that the optimization performance of the current strategy evaluated by the maximum fitness value is nearly the same as the original algorithm, verifying its good performance on optimization objectives. The optimization performance loss is merely 1% compared with the NSGA-II, which is quite satisfactory.

TABLE 5. The comparison of the strategy in the paper with previous researches.

Method	the number of total iterations
optimization strategy in this paper	38
NSGA-II algorithm	68
PSO method in reference [15]	1000
MORPSO method in reference [16]	150

Due to different optimization scenarios, it is not feasible to compare directly the optimization performance between the current strategy and the previous methods. Nevertheless, we are able to compare the number of iterations required for convergence as shown in Table 5. It is seen that the proposed strategy outperforms all the other strategies in terms of reducing the iterations, which is due to the simplification brought by the dimension reduction model. Thus, it can be concluded that this optimization strategy has successfully accelerated the convergence rate of the WPT system and improved the iteration time with acceptable loss in optimization performance.

IV. EXPERIMENTAL VERIFICATION

A case experiment with two identical extended coils is performed to experimentally validate the simulation results. It should be noting that the results of the iterative process of optimization parameters in the simulation can not be verified due to the randomness of mutation. Therefore, this section mainly verifies the correctness of dimension reduction results and optimal parameters in optimization results by evaluating the optimization objectives and fitness function.

Following the model designated in Section III A and the results of the sensitivity analysis in Section III B 2), the length, width and thickness of the ferrite and aluminum plate $b_1 \sim b_3$ and the coil parameter Z_1 have lower sensitivity, so the experiment fixes them to a constant value. Similar to Table 1, the outer diameter and width a_1, a_2 of the coil are set to be substantially same as the length and width b_1, b_2 of the ferrite and the aluminum plate. Table 6 gives the range of optimization parameters and constant parameters. The AC input voltage is the same as the variable U defined in Figure 1. According to equation (6), the value of U will not affect the optimization of kQ optimization target, but according to the electromagnetic field theory, the value of U will affect the value of electromagnetic field. However, the optimization method in this paper can be applied to different values of U, that is, the different values of U will not affect the optimization scheme and results in this paper. Therefore, typical value of U is adopted in the experiment in this paper.

Figure 10 is an experimental diagram of the coil constructed in accordance with Figure 3. The coil, ferrite and aluminum plate is constructed in terms of the simulation structure, and the dimensions are assigned as values in Table 6. The transmitter coil adopts a coil winded by a coil frame independently invented by the laboratory, which can credibly cooperate with the change of the coil spacing d to realize the optimization verification. The secondary coil is structured in a fixed structure and maintain unchanged.

TABLE 6. The design parameters of the coils to be optimized and their restrictions.

optimization parameters	Min/Max	Constant parameters	Value
Coil turn spacing: d	10.1mm/ 12mm	resonant frequency f	85kHz
		length of ferrite b_1	600mm
		width of ferrite b_2	500mm
		thickness of ferrite:b_3	5mm
		external diameters length of coil: a_1	600mm
		external diameters width of coil: a_2	500mm
distance of ferrite from coil: Z_2	0.1mm/ 5mm	coil spacing: Z_1	190mm
		AC input voltage: $V(V_{rms})$	5V
		coil turns: n	8
		radius of wire: a	2.5mm

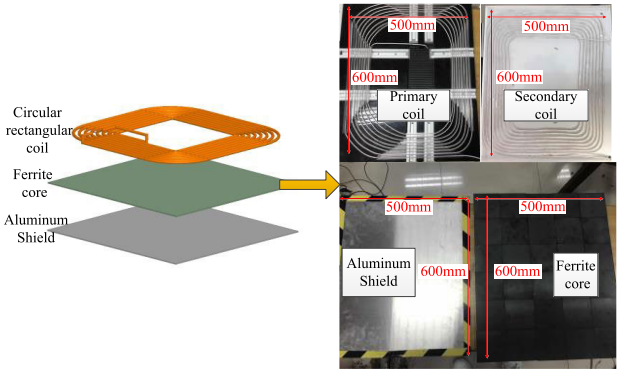

FIGURE 10. Physical winding diagram of the coil system.

In order to observe the optimization objective kQ_1Q_2 and E, the experiment utilize LCR meter 3522-50 LCR HiTESTER (HioKi E.E. Corporation, Nagano Prefecture, Japan) to implement the measurement of kQ_1Q_2 and an electric field probe EHP-50G (Narda, Segrate, Italy) with specialized computer to measure the E of space. In addition, it also includes high frequency power source, coil system (including transmitter and receiver coil, ferrite core, aluminum shielding), compensation capacitor, AC resistance load, oscilloscope, current detector, voltage detector and isolating probe. Complete set of experimental measurement equipment distribution is displayed in Figure 11.

To highlight the consistency between simulation and experiment, we adjust the input source to control the primary input voltage to maintain 5V (RMS). The oscilloscope, voltage detector and current detector are operated to capture the original secondary voltage and primary current waveform under the basic parameters as shown in Figure 12(a). The specialized computer result example is illustrated as Figure 12(b) and further results are omitted.

As shown in Figure 13, the optimization parameter d is changed by adjusting the baffle plate of the transmitter coil frame invented by the laboratory, and the Z_2 is increased by adding a thin plastic sheet.

It should be noted that in the actual experiment, the spatial electric field strength varies in accordance with the human induced electric field E and the two trends are basically no

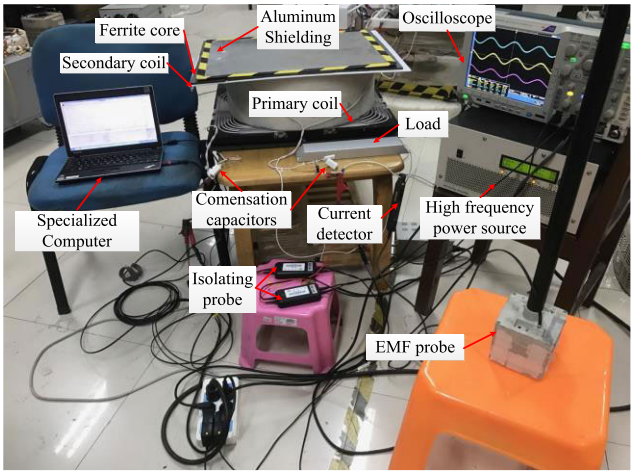

FIGURE 11. Experimental measurement equipment for multi-objective optimization test.

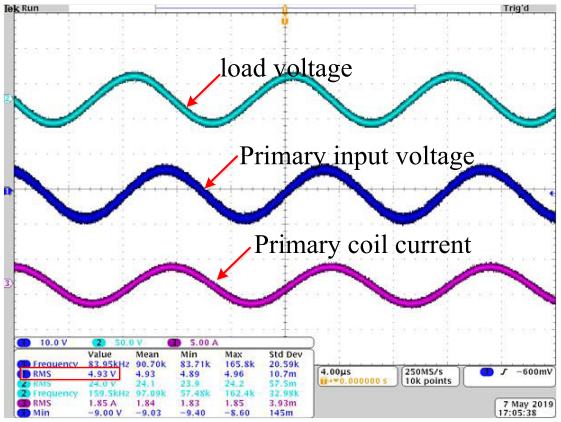

(a) Primary and secondary voltage and primary current waveform under basic parameters

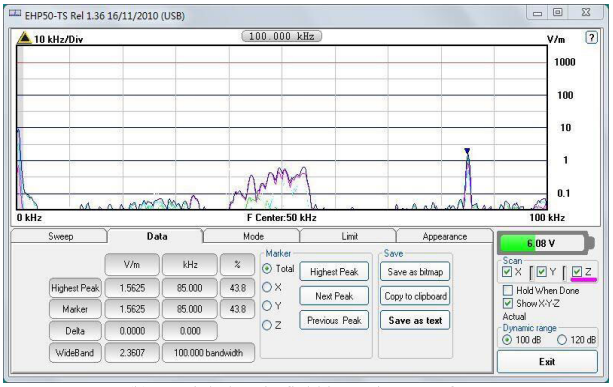

(b) Spatial electric field intensity waveform

FIGURE 12. Experimental waveforms for measuring optimization result.

discrepancy. Therefore, the spatial electric field strength can replace E to observe the variation trend during the experimental test. To verify the simulation results, d and Z_2 are respectively changed. The relationship between optimization objectives and optimization parameters d, Z_2 is recorded. Q_N and E_N represent the corresponding measured values when applying basic parameters in Table 6. Test results are recorded in Figures 14 and 15.

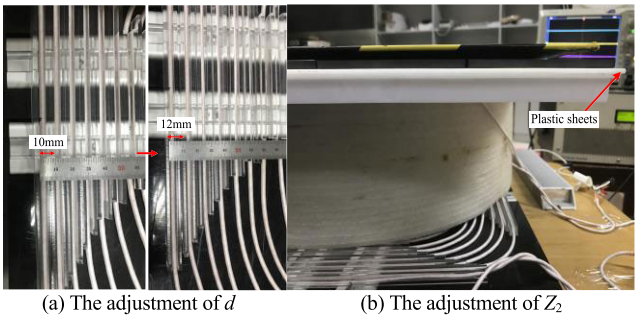

(a) The adjustment of d (b) The adjustment of Z_2

FIGURE 13. Experimental optimization parameters adjustment method.

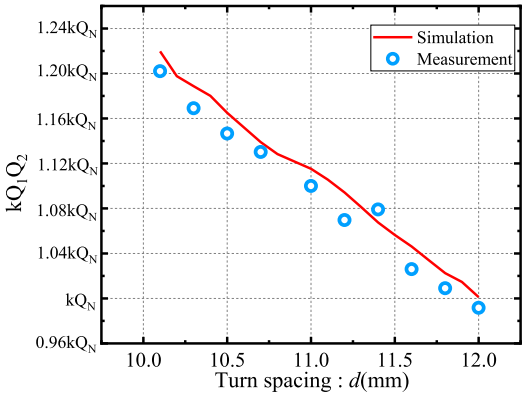

(a) Optimization parameter d

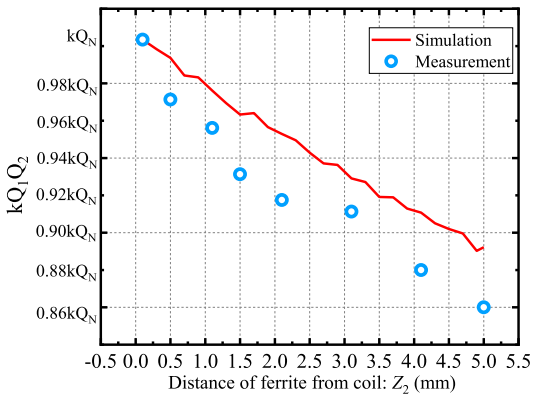

(b) Optimization parameter Z_2

FIGURE 14. Experimental verification of optimization objective kQ1Q2 sensitivity analysis results.

Figure 14 and Figure 15 demonstrate that after unifying the corresponding Q_N and E_N under the basic size parameters of experimental system and simulation system, the corresponding tendency of the experimental measurement value is consistent with the simulation whether the objective is kQ_1Q_2 or E, effectively verifying the correctness of the sensitivity analysis. However, it can be observed that there is discrepancy in Figure 14(b) between experimental measurement values and simulation value. The reason can be derived from the waveform diagram in Figure 12(a). The operating frequency of the experimental test is smaller than the simulation value due to the experimental deviation, and kQ_1Q_2 is proportional to ω^2, so the experimental measurements will be slightly

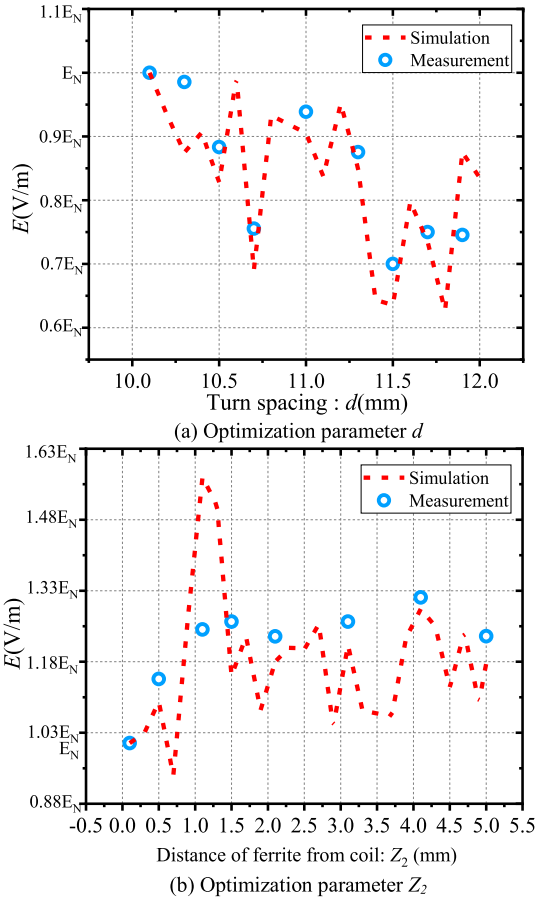

FIGURE 15. Experimental verification of optimization objective E sensitivity analysis results.

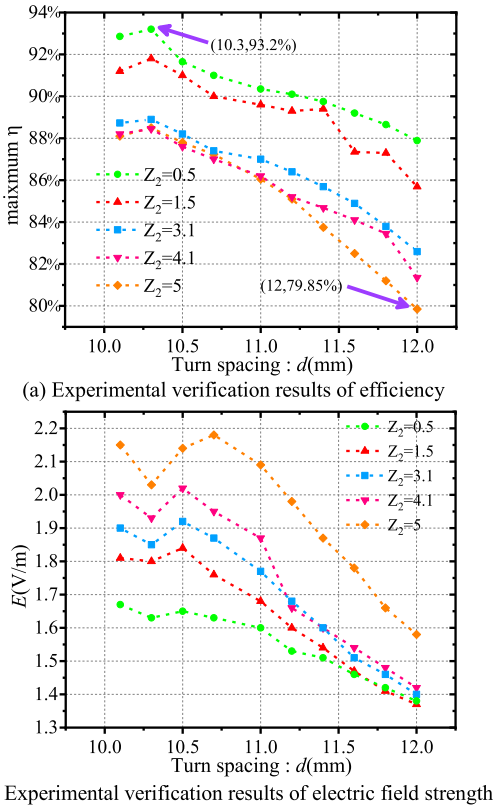

FIGURE 16. Experimental verification of optimal parameters.

smaller than the simulation values. As for the optimization target E, the tendencies of experiment and simulation are basically consistent. When d increases, the value of E generally performs a downward trend. When Z_2 increases, the value of E has a tendency to rise firstly and then stabilize. Therefore, the correctness of the dimension reduction results can be ensured.

Further experimental tests are conducted to validate the optimal parameters in optimization results. According to equation (6), the maximum efficiency η is directly related to kQ_1Q_2, and equation (6) is used to measure the maximum efficiency of WPT system corresponding to the load value in equation (5). Therefore, the corresponding load matching technology is employed to measure the maximum efficiency. The maximum efficiency and the E value of space electric field corresponds to the simulation position under each parameter are measured to evaluate the optimal optimization parameters $(d,\ Z_2) = (10.3\text{mm},0.4\text{mm})$ which are shown in Figure 16. Other design constant parameters are structured according to Table 6.

Figure 16 indicates that the maximum efficiency of the system and E can be optimized by the adjustment of d and Z_2. It can be seen from Figure 16(a) that the maximum efficiency point is maintained at $(d, Z_2) = (10.3\text{mm},0.5\text{mm})$ which is basically consistent with the optimal parameters (10.3mm,0.4mm). Due to the limitation of measurement conditions, Z_2 value is slightly deviated within the acceptable range. For electric field strength E, when Z_2 is 0.5, the value of E displays lowest, and when $d = 10.3$, the value of E is slightly reduced in range [10mm,10.5mm]. The fitness function values of all test parameters in the experiment situation are calculated. The fitness value of (10.3mm,0.5mm) is maximum values of all test parameters which is 0.931, and the value is slightly lower than simulation due to the deviation of actual parameters. The results verify the correctness of the optimization strategy.

In summary, the efficiency can be availably increased from the lowest 79.85% to the highest 93.2% with the optimization strategy of this paper, and the electric field strength E can be restrained to some extent. The correctness of the optimization strategy is verified and the experiment proves that the optimization strategy in this paper can quickly find optimal parameters in coil design without repeating test experiments. Through the optimization strategy of this paper, the WPT coil system can be optimized without clear formula and the number of trials can be reduced.

V. CONCLUSION

This paper is aimed to solve the problem of fast multi-objective optimization without a clear objective calculation formula for complex multi-parameter WPT resonant systems. An optimization strategy based on dimension

reduction method is proposed to realize fast convergence with a good optimization performance.

Our research illustrates that through the dimension reduction model based on the sensitivity analysis, the iteration time required for system convergence has been reduced by nearly 44% while maintaining almost the same optimization performance as the original algorithm. The dimension reduction results and optimal parameters are verified experimentally. The maximum efficiency of the WPT system has been shown to increase from the lowest 79.85% to the highest 93.2% and the electric field strength reduce notably. It is emphasized that the proposed optimization strategy is not confined to the present system, and it sheds a light on the optimal design of more general WPT systems. Therefore, the optimization strategy based on efficiency and safety indicators can facilitate the design of complex WPT systems and lay the foundation for its wider application.

REFERENCES

[1] S. Y. R. Hui, W. Zhong, and C. K. Lee, "A critical review of recent progress in mid-range wireless power transfer," *IEEE Trans. Power Electron.*, vol. 29, no. 9, pp. 4500–4511, Sep. 2014.

[2] A. Kurs, A. Karalis, R. Moffatt, J. D. Joannopoulos, P. Fisher, and M. Soljačić, "Wireless power transfer via strongly coupled magnetic resonances," *Science*, vol. 317, no. 5834, pp. 83–86, 2007.

[3] G. A. Covic and J. T. Boys, "Modern trends in inductive power transfer for transportation applications," *IEEE J. Emerg. Sel. Topics Power Electron.*, vol. 1, no. 1, pp. 28–41, Mar. 2013.

[4] A. O. Hariri, T. Youssef, A. Elsayed, and O. Mohammed, "A computational approach for a wireless power transfer link design optimization considering electromagnetic compatibility," *IEEE Trans. Magn.*, vol. 52, no. 3, pp. 1–4, Mar. 2016.

[5] J. L. Villa, J. Sallán, A. Llombart, and J. F. Sanz, "Design of a high frequency inductively coupled power transfer system for electric vehicle battery charge," *Appl. Energy*, vol. 86, no. 3, pp. 355–363, Mar. 2009.

[6] S. Hasanzadeh, S. Vaez-Zadeh, and A. H. Isfahani, "Optimization of a contactless power transfer system for electric vehicles," *IEEE Trans. Veh. Technol.*, vol. 61, no. 8, pp. 3566–3573, Oct. 2012.

[7] H.-J. Song, H. Shin, H.-B. Lee, J.-H. Yoon, and J.-K. Byun, "Induced current calculation in detailed 3-D adult and child model for the wireless power transfer frequency range," *IEEE Trans. Magn.*, vol. 50, no. 2, pp. 1041–1044, Feb. 2014.

[8] S. W. Park, K. Wake, and S. Watanabe, "Incident electric field effect and numerical dosimetry for a wireless power transfer system using magnetically coupled resonances," *IEEE Trans. Microw. Theory Techn.*, vol. 61, no. 9, pp. 3461–3469, Sep. 2013.

[9] A. Christ, M. G. Douglas, J. M. Roman, E. B. Cooper, A. P. Sample, B. H. Waters, J. R. Smith, and N. Kuster, "Evaluation of wireless resonant power transfer systems with human electromagnetic exposure limits," *IEEE Trans. Electromagn. Compat.*, vol. 55, no. 2, pp. 265–274, Apr. 2013.

[10] T. Shimamoto, I. Laakso, and A. Hirata, "Internal electric field in pregnant-woman model for wireless power transfer systems in electric vehicles," *Electron. Lett.*, vol. 51, no. 25, pp. 2136–2137, 2015.

[11] N. Srinivas and K. Deb, "Muiltiobjective optimization using nondominated sorting in genetic algorithms," *Evol. Comput.*, vol. 2, no. 3, pp. 221–248, 1995.

[12] K. Deb, A. Pratap, S. Agarwal, and T. Meyarivan, "A fast and elitist multiobjective genetic algorithm: NSGA-II," *IEEE Trans. Evol. Comput.*, vol. 6, no. 2, pp. 182–197, Apr. 2002.

[13] M. A. Hassan, N. Hailat, N. Badawi, and A. A. Hussein, "A wireless power transfer system with optimized circuit parameters using genetic algorithm," in *Proc. 8th Int. Renew. Energy Congr. (IREC)*, Amman, Jordan, 2017, pp. 1–4.

[14] T. Sasatani, Y. Narusue, Y. Kawahara, and T. Asami, "Genetic algorithm-based design of receiving resonator arrays for wireless power transfer via magnetic resonant coupling," in *Proc. IEEE Wireless Power Transf. Conf. (WPTC)*, Aveiro, Portugal, May 2016, pp. 1–4.

[15] N. Hasan, T. Yilmaz, R. Zane, and Z. Pantic, "Multi-objective particle swarm optimization applied to the design of wireless power transfer systems," in *Proc. IEEE Wireless Power Transf. Conf. (WPTC)*, Boulder, CO, USA, May 2015, pp. 1–4.

[16] T. Yilmaz, N. Hasan, R. Zane, and Z. Pantic, "Multi-objective optimization of circular magnetic couplers for wireless power transfer applications," *IEEE Trans. Magn.*, vol. 53, no. 8, Aug. 2017, Art. no. 8700312.

[17] F. Mach, "Reduction of optimization problem by combination of optimization algorithm and sensitivity analysis," *IEEE Trans. Magn.*, vol. 52, no. 3, Mar. 2016, Art. no. 7003104.

[18] L. Yang, S. L. Ho, and W. N. Fu, "Design optimizations of electromagnetic devices using sensitivity analysis and tabu algorithm," *IEEE Trans. Magn.*, vol. 50, no. 11, Nov. 2014, Art. no. 7201204.

[19] Z. Mengrneng, S. Qunli, and L. Long, "General reactive power optimization of distribution network based on power loss sensitivity analysis," in *Proc. 25th Chin. Control Decis. Conf. (CCDC)*, Guiyang, China, 2013, pp. 566–570.

[20] N. Rohadi and R. Živanovic, "Sensitivity analysis of a fault impedance measurement algorithm applied in protection of parallel transmission lines," in *Proc. 9th IET Int. Conf. Adv. Power Syst. Control, Operation Manage. (APSCOM)*, Hong Kong, 2012, pp. 1–6.

[21] C. C. Mi, G. Buja, S. Y. Choi, and C. T. Rim, "Modern advances in wireless power transfer systems for roadway powered electric vehicles," *IEEE Trans. Ind. Electron.*, vol. 63, no. 10, pp. 6533–6545, Oct. 2016.

[22] J. Shin, S. Shin, Y. Kim, S. Ahn, S. Lee, G. Jung, S.-J. Jeon, and D.-H. Cho, "Design and implementation of shaped magnetic-resonance-based wireless power transfer system for roadway-powered moving electric vehicles," *IEEE Trans. Ind. Electron.*, vol. 61, no. 3, pp. 1179–1192, Apr. 2014.

[23] International Commission on Non-Ionizing Radiation Protection, "Guidelines for limiting exposure to time-varying electric, magnetic, and electromagnetic fields (up to 300 GHz)," *Health Phys.*, vol. 4, pp. 494–522, Apr. 1995.

[24] International Commission on Non-Ionizing Radiation Protection, "Guidelines for limiting exposure to time-varying electric, magnetic, and electromagnetic fields (up to 300 GHz) (1 Hz To 100 kHz)," *Health Phys.*, vol. 4, pp. 818–836, Dec. 2010.

[25] I. M. Sobol, "Global sensitivity indices for nonlinear mathematical models and their Monte Carlo estimates," *Math. Comput. Simul.*, vol. 55, nos. 1–3, pp. 271–280, 2001.

[26] A. Konak, D. W. Coit, and A. E. Smith, "Multi-objective optimization using genetic algorithms: A tutorial," *Rel. Eng. Syst. Saf.*, vol. 91, no. 9, pp. 992–1007, Sep. 2006.

[27] H. Li and Q. Zhang, "Multiobjective optimization problems with complicated Pareto sets, MOEA/D and NSGA-II," *IEEE Trans. Evol. Comput.*, vol. 13, no. 2, pp. 284–302, Apr. 2009.

[28] J. Schneider, "Wireless power transfer for light-duty plug-in/electric vehicles and alignment methodology," SAE Tech. Paper J2954, 2017.

[29] C. Liu, C. Jiang, and C. Qiu, "Overview of coil designs for wireless charging of electric vehicle," in *Proc. IEEE PELS Workshop Emerg. Technol., Wireless Power Transf. (WoW)*, Chongqing, China, May 2017, pp. 1–6.

[30] *Electric Vehicle Wireless Power Transfer (WPT) Systems. Part 1—General Requirements*, Standard IEC 61980-1:2015, International Electrotechnical Commission, 2015, pp. 20–65.

[31] *Electrically Propelled Road Vehicles—Magnetic Field Wireless Power Transfer—Safety and Interoperability Requirements*, Standard ISO/PAS 19363:2017, 2017, pp. 2–59.